# Significance of homogeneous operation in light-assisted fixed-bed bioprocess under ammonia stress: Optimization, long-term operation and metagenomic analysis

Yunxin Zhu[a], Yujia Chen[a], Guangqi An[a], Cheng Zhang[a], Jingwei Yang[a], Rongyong Yang[b], Guoping Chen[c], Yingnan Yang[a]*

[a]*Graduate School of Life and Environmental Science, University of Tsukuba, 1-1-1 Tennodai, Tsukuba, Ibaraki 305-8572, Japan*

[b]*Shanghai High Victory Science and Technology Co., Ltd., 4688 Jinshan Avenue, Shanghai 201512, China*

[c]*Research Center of Functional Materials, National Institute for Materials Science,1-1 Namiki, Tsukuba, Ibaraki 305-0044, Japan*

* Corresponding author:

Tel/Fax: +81 29 8534650

E-mail address: yo.innan.fu@u.tsukuba.ac.jp (Y.Yang)

## Abstract

Activating microbes with light is a promising strategy for addressing ammonia-stressed anaerobic digestion (AD). However, as a critical in-process parameter, homogenous operation, in light-assisted AD amended by bio-fixed bed has received limited attention. This research endeavors to establish a uniform-illuminated biosystem and assess its practical feasibility through a 90-day semi-continuous operation at pilot scale under solar light illumination. The proposed system with an optimal stirring mode (intermittent stirring for 3 minutes every 15 minutes) demonstrated a robust methane yield of 914−971 mL/(g-$DOC_{removal}$·d) across various organic loads, accounting for 88.7−94.3% of the theoretical one under ammonium-rich condition (3500 mg/L). The metagenomic analysis revealed that the uniform illumination induced synergistic effects of a diverse microbial consortium, the promotion of carbohydrate and methane metabolism, and the formation of an electroactive bio-cluster for enhanced digestion. With the implementation of solar light, this study offers an easy-operated approach for sustainable waste-to-energy recovery in scale-up application.



**Keywords:** Light-assisted anaerobic digestion (AD), Ammonia inhibition, Homogenous operation, Pilot-scale evaluation, Bioinformatics analysis

## 1. Introduction

Anaerobic digestion (AD) stands out as a widely applied approach for waste control and bioenergy production (i.e., $H_2$, $CH_4$), aligning with the goals of sustainable development (Bose et al., 2021). While the ammonia inhibition that commonly occurs in AD treating nitrogen-rich waste, impairs the treatment efficiency with the restrained microbial productivity (Rajagopal et al., 2013). To address this challenge, the combination of bio-zeolite fixed-bed system with light stimulation has been proposed to enhance $CH_4$ production (Zhang et al., 2016; Zheng et al., 2020; Zhu et al., 2021). The bio-zeolite fixed-bed demonstrated notable capabilities in ammonia absorption and microbial fixation, and the employment of light stimulation could effectively promote the microbial activity and biomass growth, facilitating the biofilm formation to counteract the ammonia toxicity. Moreover, natural sunlight could be adopted to further highlight the easy-operability and sustainability of this system, making it highly promising for practical applications.

Considering the scale-up impact of an illuminated biosystem, the light availability need to be carefully controlled, as it generally influences the microbial metabolisms and biomass growth (Rossi et al., 2020). However, the limitations of sludge sedimentation and turbid mud commonly affect the light transmittance (Kariyama et al., 2018), potentially hindering the transfer of light stimulus and photo-enhancement efficiency in scaled-up reactors. Notably, in light-assisted system, *Methanosarcina* with high light affinity (Qian et al., 2022; Tada et al., 2006; Zhu et al., 2022), typically resides at the

bottom of static reactors (Kariyama et al., 2018), which makes them less accessible to light and thereby weakening the photo-stimulation efficiency. Therefore, achieving a uniform light regime is essential for effective microbial stimulation and stable performance of the developed system. As a commonly employed homogenization technique, stirring, plays an influential role in influencing the mass transfer, the contact between microbes and substrates, the stability of microbiome, the formation of biofilm, the hydrolysis/fermentation rate, and so on (Karim et al., 2005; Lindmark et al., 2014b). It may also assist to avoid the sludge sedimentation and homogenize the distribution of microbial community in lighted system, achieving a uniform environment for light stimulation. Though traditionally, stirred tank digesters operated as continuous stirred tank reactors (CSTRs), the high operational and maintenance cost of continuous stirring (~54% of energy demand for system operation) restrained the energy production efficiency (Lindmark et al., 2014a). Moreover, continuous stirring shear might lead to the destruction of microbial flocs, the detachment of biomass, resulting in the long-term upsets in large-scale application (Karim et al., 2005). Therefore, an appropriate homogenization operation should be proposed for not only maximizing the energy production but also minimizing the capital and operational costs.

Compared to no stirring and continuous stirring (CS), the economics of AD could be improved by intermittent stirring (IS). Ideal IS could realize the homogenous introduction of the fresh feed and intimate contact between the bacteria, meanwhile reduce the shear impact and energy demand caused by CS (Kariyama et al., 2018).

Suitable IS duration may also provide a uniform platform for the syntrophic association among bacteria and methanogens with favorable extracellular polymeric substances (EPS) production for resisting ammonia stress (Bose et al., 2021; Ong et al., 2002). Moreover, IS may impact the community structure and formed microbial layer. Methanogens with long-rod structure (i.e., acetoclastic *Methanosaeta*) are generally sensitive to continuously stirring, while a good balance of *Methanosaeta* and *Methanosarcina* could be achieved in the intermittent mixed digesters (Kariyama et al., 2018). Therefore, optimizing IS strategy is prerequisite for achieving a uniformly illuminated consortia with efficient AD performance under ammonia stress. Until now, existing studies mainly focused on the stirring effect in dark AD, leading to a lack of experience regarding the homogenization of both the nutrients and light distribution in illuminated bioreactor, especially under ammonia inhibition. Moreover, there have been no report on the practical applicability of lighted AD system in terms of scale-up implementation, long-term stability and solar assistance. Besides, the combined effect of homogeneous operation and light stimulation on microbial communities and metabolic pathways remains unclear.

Therefore, this research aimed to develop a homogenous-illuminated biosystem for efficient ammonia-rich AD by optimizing stirring operation. The practical applicability of proposed system was evaluated through a 3-month pilot-scale operation with simulated solar light as light source. Finally, bioinformatics analysis delved into the mechanisms underlying microbial communities, metabolic pathways, and biofilm

characteristics. This study provides a guide for establishing a sustainable waste management system with efficient bioenergy recovery for scale-up application.

## 2. Materials and methods

### 2.1. Seed sludge, feedstock and fixed-bed biosystem

The original seed sludge was regularly sourced from an anaerobic digester at a full-scale mesophilic wastewater treatment plant handling municipal wastewater (Ibaraki prefecture, Japan). Subsequently, it was separated, sealed and refrigerated (4℃) before pre-culturing. Following a two-week acclimatization at 55℃ with a synthetic medium (glucose (2.5 g/L), sodium acetate (2.5 g/L), $KH_2PO_4$ (16 mg/L), yeast extract (200 mg/L), and a trace mineral solution (5% v/v), the cultured inoculum was prepared for batch and semi-continuous assays. The chemical composition of synthetic medium and the pre-culturing method were documented in previous study (Zhu et al., 2022). Fermentation assays were conducted in a bio-zeolite fixed-bed reactor (Zhang et al., 2016), utilizing a 330 $cm^2$/L porous nylon bag (H-[HN($CH_2$)XCO]–OH, T&T, Kainan, Japan) as fixed material filled with 10 g/L zeolite A-3 (Wako Pure Chemical Industries, Ltd.) for microbial immobilization and ammonia absorption (See Supplementary Materials).

### 2.2. Exploration of optimal stirring condition for light-assisted anaerobic bioreactor under ammonia stress

AD batch experiments were conducted in bio-zeolite fixed-bed bioreactors (effective working volume of 200 mL, SIBATA) with synthetic medium and

acclimatized inoculum at a ratio of 4:1 (v/v) under thermophilic condition (55 ± 1℃). $NH_4Cl$ was adopted in each reactor to simulate an ammonia-stressed environment (3000 mg $NH_4^+$-N/L). The initial pH of 7.0 ± 0.2 was adjusted using 1 M NaOH and 1 M HCl before imparting the anaerobic condition. Daily incandescent lamp illumination (400−800 nm, LW110V60W, Mitsubishi Ashram, Tokyo, Japan) was applied to lighted reactors (marked as 'L') with the optimal light condition of photon number ($N_R$) $=1.25\times10^4$ μmol/(day·L) with 34 μmol/($m^2$·s) for 90 min/day (Zhu et al., 2021).

To investigate the effect of homogenization on light-assisted system, a magnetic stirrers (SW-M60, NISSIN) with a stirring speed of 100 rpm was applied based on previous studies (Li et al., 2022; Liu et al., 2024). Preliminary experiments determined suitable stirring modes for lighted reactors during 90-minute illumination (See Supplementary Materials), including no-stirring (L), constant stirring for 90 mins (L-CS) and intermittent stirring with 1 min stirring in every 15 min (L-IS1). Dark reactors with the same stirring modes served as controls (D, D-CS, D-IS1, respectively). Enhanced methanogenic productivity in the L-IS1 group indicated the advantage of intermittent stirring over constant stirring and no stirring in the developed lighted reactor (See Supplementary Materials). To optimize the IS condition, reactors were operated with different stirring durations of 1, 3, 5, 7 min in every 15 min during 90-min illumination, labeled as L-IS1, L-IS3, L-IS5, L-IS7, respectively. Each group was performed in triplicate for 9 days.

## 2.3 Long-term effectiveness of homogenous-illuminated system at pilot scale

To assess the practical efficacy of the optimal stirring condition, a polit-scale semi-continuous AD digester (MDL-10L, B.E.Marubishi) was established (See Supplementary Materials). The digester equipped with a double-layered six-blade propeller device for stirring, and an automatic controlling system for real-time monitoring (i.e., daily biogas volume, temperature (55 ± 1℃), pH and stirring operation). Daily exchange of feedstock and fermentation broth was implemented by peristaltic pump. Initially, a specified quantity of fixed materials and zeolite was suspended in the digester (according to 8 L working volume). An ultraviolet-cut artificial solar light (370−2000 nm, XC-100, 110 V1.8A, SERIC ltd., Tokyo, Japan) was applied as light source to simulate solar illumination.

The 90-day semi-continuous operations were divided into three stages: Dark (day 0-20, dark without stirring), Light (day 21-50, light without stirring) and Light-$S_{opt}$ (day 51-90, light with optimum stirring). Operations started with batch feeding for microbial acclimatization (10 days), in which the ammonia-rich feedstock (3500 ± 100 mg $NH_4^+$-N/L) and inoculum were initially fed to reactors on day 0. From day 11, the digester was fed in semi-continuous mode with organic load rate (OLR) of 0.19 g-$DOC_{added}$/(L·d) and hydraulic retention times (HRT) of 10 days. Specifically, 800 mL of ammonia-rich synthetic medium was exchanged with the same volume of effluent. From day 21, intermittent illumination was introduced to reactor using artificial solar light. From day 51, the proposed optimal stirring condition was applied to the illuminated digester

during daily illumination. After a 20-day stabilization period, the OLR was increased to 0.34 and 0.71 g-$DOC_{added}$/(L·d) (during day 71-80 and day 81-90, respectively) with shorter HRT (5 days), to evaluate the capacity of proposed homogeneous-illuminated system.

## 2.4 Analytical methods

Biogas was collected daily, and every other day, 10 mL of the sampled digestate underwent centrifugation for further analysis. The biogas composition, total solid content (TS), volatile solids content (VS), dissolved organic carbon (DOC), volatile fatty acids (VFAs), ammonium nitrogen, pH during fermentation was measured following a previous protocol (Zhu et al., 2021). The precipitate of the sludge sample was utilized for assessing the following indicators. Adenosine triphosphate (ATP), coenzyme $F_{420}$ and sludge conductance were measured according to previous study (Zheng et al., 2020). EPS was extracted from the sludge mixture using physical heat method (He et al., 2021). Briefly, the sludge samples were centrifuged (4000 g for 10 min, 4ºC) and the obtained supernatants were filtered through 0.45 μm membrane filter, serving as dissolved organic matters (DOM). The residue in the centrifuge tube was then suspended to the original volume with distilled water, sheared by a vortex mixer for 1 min, and loosely bound EPSs (LB-EPSs) were extracted using the same centrifugation process. Finally, the residue was used to extract tightly bound EPSs (TB-EPSs) through heating (60℃, 30 min) in a water bath. The collected supernatants after each centrifugation were filtered through a 0.45 μm membrane for total organic carbon

(TOC) analysis. To evaluate the long-term performance under different operation conditions, the theoretical bio-$CH_4$ yield ($BMY_{thDOC}$) was calculated based on the experimental DOC of the substrate (mL/g-$DOC_{added}$), according to previous study (Zhu et al., 2021).

**2.5 Microbial community analysis**

The samples for DNA analysis were collected at the end of the characteristic fermentation period of Dark, Light, and Light-$S_{opt}$, and quick frozen at -80℃. Illumina MiSeq paired-end sequencing (Illumina, USA) of 16S rRNA V4 regions (515F-806R) was performed at Bioengineering Lab. Co., Ltd. (Kanagawa, Japan). Quality filtered reads were assigned to operational taxonomic units (OTUs) using taxonomic assignment against the EzBioCloud 16S database (https:// www. ezbiocloud. net/) (Yoon et al., 2017). Indices of α-diversity for richness comparison (observed species and Chao1 index) and diversity comparison (Shannon index and phylogenetic diversity (PD) whole tree) were normalized using sequences (no less than 10000 sequences) obtained among different samples. Functional prediction analysis was performed via PICRUSt2 (Phylogenetic Investigation of Communities by Reconstruction of Unobserved States), to evaluate the expression of key metabolic pathways based on 16S rRNA data. The KEGG (Kyoto Encyclopedia of Genes and Genomes) database was used to support functional gene profiling (https://www.genome.jp/kegg/mapper/).

### 2.6 Kinetic and statistical analyses

The $CH_4$ production data from the batch experiment were fitted to the modified Gompertz model (Liu et al., 2022) using IBM SPSS statistics (Stats Guild Inc., Japan). One way Analysis of Variance (ANOVA) followed by t-test with a threshold value of 0.05 on experimental data was performed to evaluate the statistical significance of the results. Principal component analysis (PCA) and cluster analysis were conducted using Origin 2021 software.

## 3. Result and discussion

### 3.1 Optimal stirring condition for lighted system under ammonia stress

The performance of ammonia-rich AD under various intermittent stirring conditions was illustrated in Fig. 1a. The cumulative $CH_4$ productions of L (408 ± 15 mL/L), L-IS1 (447 ± 18 mL/L), L-IS3 (483 ± 19 mL/L), L-IS5 (383 ± 19 mL/L) were 1.44, 1.58, 1.71 and 1.35 folds of dark control (283 ± 21 mL/L), respectively. While L-IS7 exhibited a similar performance (295 ± 15 mL/L) to the dark group. This result suggested that light stimulation coupled with proper homogeneous operation, might synergistically enhance the methanogenic productivity under ammonia stress. Based on experimental data, three major kinetic parameters, i.e., maximum cumulative $CH_4$ production ($M_{max}$), maximum $CH_4$ production rate ($R_{max}$), and lag-phase time ($\lambda$, d) were further predicted from the Gompertz model with good fit ($R^2 = 0.983-0.995$) (Fig. 1b). Besides, cumulative $CH_4$ production in L-IS3 reached a plateau 1 day earlier than the light control (Fig. 1a), indicating that intermittent string could shorten the start-up

period and digestion time under ammonia stress. As the stirring period increased to 3 min, $M_{max}$ (490 ± 8 mL/L) peaked in L-IS3 with the shortest λ (0.8 d) and fast $R_{max}$ (198 mL/(L·d)). But when the stirring time further ascending to 7 min, $M_{max}$ and $R_{max}$ sharply decreased to 302 mL/L and 111 mL/(L·d), which were even lower than that of light control. Consequently, 3-min intermittent stirring contributed to the highest $CH_4$ yield of 372 ± 21 mL/(g-$DOC_{removal}$·d) in the homogeneous-illuminated system (L-IS3), which was 1.57 folds and 1.25 folds of dark (191 ± 14 mL/(g-$DOC_{removal}$·d)) and light control (299 ± 15 mL/(g-$DOC_{removal}$·d)), respectively (Fig. 1c). Whereas further prolonging the stirring duration to 7 mins (L-IS7) could decrease the $M_{max}$ and $CH_4$ yield by 28% and 34% as compared to that of light control. The significance of optimized intermittent stirring for effective digestion demonstrated in this study, was in aligned with previous studies (Bose et al., 2021), suggesting that intermittently minimal stirring period could shorten the acclimatization period, accelerate the biogas generation rate and maximize the digestion performance.

To further explore the potential synergy of optimal stirring and light stimulation, ATP and coenzyme $F_{420}$, as indicators of microbial activity and methanogenic productivity, were analyzed (Fig. 1d). All illuminated reactors exhibited higher ATP values than that of the dark control. The highest ATP concentration was obtained in L-IS3 (5.78 ± 0.31 μmol/L), leading to 20% and 67% increment compared to L (4.81 ± 0.17 μmol/L) and D (3.46 ± 0.29 μmol/L), respectively. ATP, as the intracellular energy currency, drives the cellular processes and positively associates with bioprocess

efficiency (Zhu et al., 2022). The higher ATP value observed in L-IS3 indicated that well-uniformed activation of ammonia-stressed anaerobes was achieved by proper intermittent. Similar stimulating effects on methanogenic activity could also be found in L-IS3, where the highest coenzyme $F_{420}$ (0.70 ± 0.07 μmol/L) was obtained. Coenzyme $F_{420}$, as a unique enzyme in methanogens, participates in the critical redox reaction of the methanogenesis (Zheng et al., 2020). The promoted coenzyme $F_{420}$ levels claimed the enrichment of methanogens and stimulated methanogenic productivity in L-IS3. However, longer stirring time in L-IS7 dramatically deteriorated the methanogenic activity with deceased coenzyme $F_{420}$ level to 0.41 ± 0.06 μmol/L, even lower than that of the dark control (0.48 ± 0.05 μmol/L). This might be associated with the destabilized methanogenic activity and structure under excessive stirring, as some filamentous methanogen (i.e., *Methanosaeta*) would be vulnerable to harsh mixing (Kariyama et al., 2018). Moreover, the ammonia inhibitory effect on methanogenic consortia could be further magnified with intensive stirring, as inappropriate mixing might obstruct the bio-cluster formation and thus restrain methanogenic activity (Bose et al., 2021).

This would be further supported by the lower sludge conductivity obtained in L-IS7 (0.37 ± 0.07 μS/cm), which decreased by 52% and 33% compared to L-IS3 (0.77 ± 0.05 μS/cm) and L (0.55 ± 0.04 μS/cm), respectively (Fig. 1e). Sludge conductivity is an index of efficiently electronical cell-cell association and biofilm formation for syntrophic growth (Zheng et al., 2020). Previous study suggested that the immobilized biomass in light-assisted fixed-bed system could promote electron ($e^-$) transfer and

enhance methanogenic performance under ammonia stress, probably due to enriched syntrophic partners and reduced interspecies distance for efficient contact (Zhu et al., 2022). However, this harmony in bio-cluster was disturbed by intensive stirring in L-IS7, leading to the reduced electroactivity and lower microbial activity. In contrast, homogenous illumination provided by L-IS3 could favor the microbial colonization for electronic syntrophic growth and relieve ammonia stress on microbial activity, contributing to efficient methanogenic productivity.

Therefore, intermittent stirring for 3 min/15 interval could be proposed as the optimal stirring strategy for developing a homogenous-illuminated fixed-bed system during ammonia-rich AD process. From a practical standpoint, the intermittently stirred digester, producing the greatest amount of $CH_4$ with minimized electrical energy consumption, could make the process more economical for scaled-up operation.

### 3.2 Capacity of the proposed homogenous-illuminated system in long-term operation at pilot scale

To validate the feasibility of proposed homogenous-illuminated system for long-term operation, a pilot-scale AD treating ammonia-rich feedstock was carried out with different OLR conditions. Though under high ammonia stress, digester successfully started up with steadily increased $CH_4$ concentration during the first 10-day operation (Fig. 2a). This could be ascribed to the advantages of fixed-bed system on microbial fixation, ammonia absorption and buffer capacity (Zhang et al., 2016; Zheng et al., 2020), which was evidenced by increased biomass quantity from 2.17 to 2.64 g VS/L

(Fig. 2a) and reduced ammonium level from 3439 to 3042 mg/L during start-up period (Fig. 2b). By amending with solar light stimulation (day 21−50), the digester could maintain stable performance with a stable $CH_4$ content (72.0 ± 2.2%) during Light stage than that of Dark stage (68.8 ± 12.7%). When homogenous operation was further introduced in Light-$S_{opt}$ stage (day 51-90), the average $CH_4$ content increased from 73.5 ± 1.9% to 72.4 ± 2.5% and 73.4 ± 2.9% with elevated OLR of 0.19 to 0.34 and 0.71 g-$DOC_{added}$/(L·d), respectively (Fig. 2a). Though HRT sharply decreased from 10 to 5 days (day 71−90), stable biomass quantity (2.28−2.37 g VS/L) could be kept in homogeneous-illuminated system without significant washout, which was ascribed to the effective immobilization of biomass. Additionally, a reduced ammonium concentration was observed in the Light-$S_{opt}$ stage (3159 ± 21 mg/L) than that of the Light stage (3200 ± 50 mg/L), suggesting that more ammonium as essential nitrogen source could be consumed by fixed anaerobes in homogenous-stimulated system.

Moreover, carbon conversion was also promoted by well-homogeneous light stimulation, as evidenced by higher DOC removal rate of 85.3% than that of Dark (80.6%) and Light (83.1%) (Table 1). With homogenous operation, organic carbon was evenly distributed and consumed by well-illuminated anaerobes, resulting in boosted $CH_4$ yield in Light-$S_{opt}$ (914 ± 31 mL/(g-$DOC_{removal}$·d)) compared to Dark (781 ± 26 mL/(g-$DOC_{removal}$·d)) and Light (877 ± 36 mL/(g-$DOC_{removal}$·d)) stages under the same OLR (0.19 g-$DOC_{added}$/(L·d)). Moreover, this well-homogenized system led to a steadily increased $CH_4$ yield to 971 ± 29 mL/(g-$DOC_{removal}$·d) at OLR of 0.71 g-$DOC_{added}$/(L·d),

covering 94.3% of theoretical $CH_4$ yield ($BMY_{thDOC}$ = 1.03 L/g-$DOC_{added}$). Generally, the ammonia-stressed AD operated in practice often faces the so-called 'inhibited steady-state' when treating degradable nitrogen-rich substrates with low C/N ratio (< 25) (Zheng et al., 2021), where the reactor was characterized with a stable performance but repressed $CH_4$ yield (34−50% of the theoretical value at ammonium level of 3000−4000 mg/L) (Nielfa et al., 2015; Zhu et al., 2021). In this study, however, 88.7−94.3% $BMY_{thDOC}$ was achieved under ammonium stress of 3500 mg/L with extremely lower C/N ratio (0.31−0.56) in the proposed homogenous-illuminated system. This result suggested the proposed system was effective to maximize the organic-to-$CH_4$ conversion under ammonia stress at pilot scale for long-term application.

To further uncover the effect of homogenous-illumination on formed anaerobic biofilm, indexes of microbial activity (ATP and coenzyme $F_{420}$) and biofilm characterizations (EPS variation and sludge conductivity) were analyzed (Fig. 2c−e). At low OLR of 0.19 g-$DOC_{added}$/(L·d), a higher ATP level was obtained in Light-$S_{opt}$ (18.1 ± 1.0 μmol/L) than that of Dark (11.9 ± 0.9 μmol/L) and Light (14.6 ± 0.8 μmol/L) (Fig. 2c), demonstrating a better microbial activity for biochemical conversion was achieved under uniform illumination. The ATP level reached a peak (24.7 ± 1.2 μmol/L) in homogenous-illuminated system when OLR increased to 0.71 g-$DOC_{added}$/(L·d). This could be ascribed to that sufficient carbon supply with homogenous operation might evenly benefit the well-activated anaerobes. Similar tendency could be found in the variation of coenzyme $F_{420}$ (Fig. 2c), where relative higher levels appeared during the

Light-S $_{opt}$ stage (ranging from 0.42 ± 0.02 to 0.45 ± 0.02 μmol/L) than that of Dark (0.36 ± 0.05 μmol/L) and Light (0.38 ± 0.03 μmol/L) stages.

Moreover, the optimized homogenization in the system provided an optimal surrounding environment to microbes for electrically syntrophic metabolism, as evidenced by doubled sludge conductance (17.6 ± 1.2 μmol/L) obtained in Light-S $_{opt}$ (0.71) stage compared to that of the Dark (0.19) stage (8.9 ± 0.7 μmol/L) (Fig. 2d). Electroactive microorganisms generally communicate with other cells or interact with external environments via $e^-$ mediators (Dang et al., 2022). Those semiconductive substances (i.e., polysaccharides, proteins, humic substances, etc.) that surrounded microbial cells consisted the EPS matrix, possessing double-layer structure, including inner-layered TB-EPS and outer-layered LB-EPS which enveloped by DOM and (Babiak and Krzemińska, 2021). Outer-layered EPS absorbed organic compounds from the surrounding environment, serving as carbon sources for biofilm. At low OLR, DOM (352 ± 16 mg-DOC/g-VS) and LB-EPS (14 ± 1 mg-DOC/g-VS) in the Dark (0.19) stage decreased to 259 ± 13 mg-DOC/g-VS and 11 ± 1 mg-DOC/g-VS when homogenous illumination was induced, respectively (Fig. 2e). This indicated that more carbon source could be consumed for biomass growth and biofilm formation, corresponding with a higher DOC removal efficiency (Table 1) with promoted biomass activity (Fig. 2c). Whereas TB-EPS quantity exhibited insignificantly change (14−15 mg-DOC/g-VS) with or without homogenous illumination. Until OLR gradually increased to 0.71 g-$DOC_{added}$/(L·d), peaked TB-EPS (22 ± 1 mg-DOC/g-VS) was observed in homogenous-

illuminated stage. TB-EPS, storing the conducting polymers, plays a vital role in extracellular $e^-$ transfer and promotes the aggregation of sludge cells. Besides, self-secreted coenzyme $F_{420}$ and amino acids were mainly detected in the TB-EPS according to (Wang et al., 2020). Accordingly, the highly secreted TB-EPS under homogenous illumination aligned with higher coenzyme $F_{420}$ bioactivity (Fig. 2c) and promoted sludge conductivity (Fig. 2d), probably related to the existence of external $e^-$ accepter or carriers. Moreover, TB-EPS quantity was found to be positively corelated with ammonia level and organic load, as it directly coats on the cell surface as a natural shell protecting cell or membrane-bound enzymes from toxics attacks (Yan et al., 2019). The intermittent homogenous operation provided anaerobes with evenly and sufficient chance to contact with substrate and each other, forming an effective biofilm for organic removal. Therefore, light stimulation with proposed homogenous operation synergistically promoted the biomass activity and quantity, methanogenic productivity and syntrophic metabolism, contributing to a stable and outperformed $CH_4$ conversion from ammonia-rich feedstock. The 90-day superior efficiency obtained from pilot-scale reactor provided a solid foundation for scaling-up application of developed system with maximal bioenergy recovery from organic waste under solar illumination.

### 3.3 Variation of microbial communities

#### 3.3.1 Effect of homogenous illumination on microbial diversity

In order to explore the synergy between light and homogenous operation on microbial consortia, 16S rRNA genes of the microbial communities from Dark, Light

and Light-S $_{opt}$ were sequenced, resulting in a total of 41450 useful sequences per sample. Fig. 3a−d depicted the alpha diversity based on effective sequences. Index of observed species (Fig. 3a), representing the number of confirmed OTUs, increased from 675 (Dark) to 743 and 972 (in Light and Light-S $_{opt}$ stage, respectively). Moreover, a higher Chao1 richness index of 1876 and 2095 was observed in Light and Light-S $_{opt}$ stages, respectively (Fig. 3b), which were 1.17-fold and 1.31-fold of Dark (1605). Those elevated indexes indicated the potential of light stimulation in increasing the microbial richness and abundance, which were further strengthened by the optimized homogenous operation. Moreover, PD whole tree and Shannon index under no-stirred darkness drastically increased from 51 and 4.0 to 66 and 4.9 under homogeneous illumination (Fig. 3c-d), respectively. PD whole tree indicates the systematic diversity by summarizing the distances in a constructed phylogenetic tree, while Shannon calculates the interspecies evenness based on the proportions of each species. The variations of two indexes suggested that the community under darkness characterized by a poor diversity could be regulated by homogenous illumination, which led to evenly distributed populations with higher diversity in Light-S $_{opt}$ stage. The balanced and diversified community structure formed under homogeneous illumination was further supported by PCA results (Fig. 3e), where *Methanosarcina* and *Methanosaeta* closely surrounded the Light-S $_{opt}$ and clustered with bacterial populations (Atribacteria OP9, Actinobacteria, Proteobacteria, Chloroflexi, Synergistetes, Atribacteria OP8 and Bacteroidetes). In contrast, Firmicutes (68% of bacterial populations) with

372 *Methanothermobacter* (85% of archaeal populations) overwhelmingly dominated during
373 the Dark stage (See Supplementary Materials). As biodiversity was crucial for the
374 longer-term resilience of ecosystem (Oliver et al., 2015), the homogenous-illuminated
375 system thereby achieved an outperformed and stable organic-to-$CH_4$ conversion under
376 high ammonia stress.

377 **3.3.2 Bacterial and archaeal structure under homogenous illumination**

378 To delve into the diverse community, we represented the bacterial structure at the
379 family level in a heat map (Fig. 4a). In Light-$S_{opt}$, a distinctive bacterial cluster
380 emerged, including OPB54 (Hydrogenispora), Rhodobacteraceae, Rhizobiales,
381 Solirubrobacterales, Actinomycetales, Atribacteria OP9_f, Anaerobaculaceae,
382 Thermotogaceae and Thermodesulfobiaceae. OPB54 (Hydrogenispora) is known for its
383 $H_2$ productivity under ammonia stress (Fischer et al., 2019) and Rhodobacteraceae and
384 Rhizobiales are related to nitrogen fixation and ammonia utilization (Tian et al., 2018).
385 Their enrichment highlighted the microbial community's adaptability to the ammonia-
386 rich condition. The filamentous Solirubrobacterales and Actinomycetales are linked to
387 organic hydrolysis and carbon removal, favoring the breakdown of complex organic
388 compounds (Haig et al., 2015). Moreover, Anaerobaculaceae specializes in VFAs
389 generation, while Atribacteria OP9_f is suggested as syntrophic propionate-oxidizing
390 bacteria that producing acetate (Dyksma et al., 2020). Thermotogaceae and
391 Thermodesulfobiaceae, as typical syntrophic acetate oxidizing bacteria (SAOB)

converts the metabolized acetate into $H_2/CO_2$ (Hattori, 2008). Notably, the presence of Thermodesulfobiaceae is commonly associated with configurations using biofilm support, corresponding to fixed-bed system used in this study (Lembo et al., 2020). In Light-$S_{opt}$, the bacterial cluster encompassed various bacterial families with specific metabolic roles, contributing to a highly cooperative and specialized microbial network. In contrast, only certain sugar fermenter (Bacillales), and $H_2$ producing bacteria (Ruminococcaceae. Clostridiaceae and Thermoanaerobacterales) were survived during the non-stirred dark period under ammonia.

Corresponded to the regulated bacterial community, archaeal community was also shifted to more balanced structure under homogenous illumination (Fig. 4b). The dominance of *Methanothermobacter* in the Dark and Light stages reduced to 54% in Light-$S_{opt}$, when the abundance of *Methanosarcina* and *Methanosaeta* increased from 9% to 35% and 3% to 7%, respectively. The former methanogen ubiquitously involves in hydrogenotrophic methanogenesis (HM), while the latter two could produce $CH_4$ via acetoclastic methanogenesis (AM), a pathway that generally accounts 60-70% $CH_4$ productivity. As reported, *Methanosarcina* spp. grow as cocci, usually shows high resistance to stressful condition, due to their versatile metabolic ability in both HM and AM. And the long-rod like *Methanosaeta* cells are sensitive to ammonia stress and intensitive mixing, and only increase in abundance when there is no VFA accumulation (Kowalczyk et al., 2013). Accordingly, homogenous illumination could effectively recover the ammonia-sensitive *Methanosaeta* meanwhile enriched the versatile

413 *Methanosarcina*, contributing to a good balance of AM and HM for efficient $CH_4$
414 production under ammonia stress.

415 **3.4 Metabolic response to homogenous light stimulation**

416 To unveil the impact of homogenous illumination on microbial metabolism,
417 bioinformatic analysis was performed based on categories in the KEGG databases. A
418 total of 19369550, 19924595 and 23605033 unique genes were predicted from the Dark,
419 Light and Light-$S_{opt}$ samples, respectively. Most detected functions were shared across
420 all the stages but were more abundant in Light-$S_{opt}$ (See Supplementary Materials),
421 indicating enhanced metabolic capabilities of the microbial community under
422 homogenous illumination. Within the Metabolism category, which governs the
423 bioconversion efficiency of AD, methane metabolism was the most abundant
424 classification, followed by energy production (Oxidative phosphorylation) as well as the
425 pathways related to carbohydrate conversion (Glycolysis and Pyruvate metabolism) and
426 organic acid degradation (Butanoate and Propanoate metabolism). The upregulated gene
427 expressions in these categories reflected the promoted metabolic activity for organics-
428 to-$CH_4$ in Light-$S_{opt}$ under ammonia stress (Fig. 5a).

429 Methanogens then consume the fermentative metabolites via AM and/or HM for
430 terminal $CH_4$ production. The genes coding for critical methanogenic reactions
431 including EC:2.7.2.1 and EC:2.3.1.8 (for acetate consumption), EC:1.5.98.2 (for $CO_2$
432 reduction) and EC:1.8.98.1 (for methanation) were more abundant in Light-$S_{opt}$ as
433 compared to Dark and Light stages (See Supplementary Materials), suggesting the

promoted dual methanogenic pathways under uniform light stimulation. Besides, genes encoding carbamoyl phosphate synthase and glutamine synthetase, which function in the protein synthesis using ammonia to constitute the microbes, were highly expressed in the Light-$S_{opt}$ stage (Fig. 5a). This result indicated that the ammonia consumption was promoted under uniformed light stimulation, aligning with the reduced ammonia levels during the Light-$S_{opt}$ stage (Fig. 2b). Therefore, the activated and carbohydrate, nitrogen and methane metabolism contributed to efficient organic-to-$CH_4$ under ammonia-rich condition.

Moreover, the successful bioconversion was fueled by intracellular energy of ATP and $e^-$, mainly producing from oxidative phosphorylation. The involved NADH: quinone oxidoreductase (M00144) acted as critical precursors for $e^-$ generation, while the F-type ATPase (M00157) and V/A-type ATPase (M00159) were responsible for ATP synthesis in bacterial and archaeal cells, respectively (Zhao et al., 2020). Gene abundances involved in the energy production were effectively upregulated in Light-$S_{opt}$ as compared to other stages (Fig. 5a), supporting the higher ATP levels observed in the Light-$S_{opt}$ stage (Fig. 2c). Furthermore, the yield of more $e^-$ flux and energy might promote electroactive species to produce the biological $e^-$ transfer components of electrically conductive pili (e-pili) and/or c-type cytochrome (Cyt C), which involved in direct interspecies electron transfer (DIET) (Dang et al., 2022). Increased gene abundances related to Cyt C and e-pili accessory proteins were detected in Light-$S_{opt}$ compared to other stages (Fig. 5b). This suggested that homogeneously illuminated

anaerobes engaged in an energy-conserving syntrophic association through extracellular $e^-$ exchange facilitated by Cyt C and e-pili. The higher conductivity observed in sludge exposed to homogeneous illumination (Fig. 2d) supported this evidence.

Additionally, the formation of DIET-dependent biofilm was reported to be highly regulated by quorum sensing (QS) system (Dang et al., 2022). With more QS system-related genes observed during Light-$S_{opt}$ stage (Fig. 5a), anaerobes in biofilm might produce more Cyt C and e-pili facilitating DIET-based syntrophic methanogenesis. Additionally, QS signals were strongly correlated with the formation of compact biofilm/aggregates accompanied with EPS production (Fig. 2e), leading to a structured conductive bio-cluster for highly efficient organic conversion.

### 3.5 Proposed mechanism and significance of results

By integrating metagenomic analysis with digestion performance, the synergistic effects of homogenous operation and light stimulation for enhanced AD performance under ammonia stress were proposed (Fig. 5c). (1) Optimal stirring strategy ensured uniform distribution of light photons in the bioreactor, and (2) facilitate efficient contacts between anaerobes and nutrients. (3) The efficient light transmittance and nutrients nourishment allowed for the even enrichment of increasing populations (Fig. 3), forming a diverse bio-cluster to resist ammonia stress. (4) Those light-activated anaerobes triggered an efficient metabolic process and syntrophic association for oragnics-to-$CH_4$ conversion. Specifically, homogenous light stimulation upregulated the carbohydrate metabolism, fatty acid degradation and ammonia consumption (Fig. 5a),

476 leading to an efficient DOC and ammonia removal during the long-term operation
477 (Table 1 and Fig. 2b). Moreover, the microbial activity and critical enzymes involved in
478 dual methanogenic pathways, particular the acetoclastic methanogenesis, were
479 significantly activated in proposed system (Fig. 5a), contributing to the boosted $CH_4$
480 yield (Table 1). Additionally, an energy-saving and kinetically faster electronic
481 association for $CH_4$ production via Cyt C and e-pili was established (Fig. 5b). This was
482 potentially ascribed to the light-enriched bio-cluster, including electroactive bacteria
483 (i.e., Anaerobaculaceae, Thermotogaceae and Thermodesulfobiaceae) and methanogens
484 (i.e., *Methanosarcina* and *Methanosaeta*) (Fig. 4). (5) With positive regulation of QS
485 signals (Fig. 5a), this close-knit cluster formed a conductive biofilm with well-
486 structured EPS (Fig. 2d−e), which assisted to promote the ammonia resistance and
487 accelerated the syntrophic metabolism for $CH_4$ production. Consequently, this
488 homogenous-illuminated community with favorable metabolic characteristics
489 contributed to outperformed and stable $CH_4$ recovery in ammonia-stressed AD during
490 long-term operation.

491 **4. Conclusion**

492 This study provided an innovative insight into the role of homogenous operation in
493 light-assisted anaerobic digester under ammonia inhibition. The synergy of intermittent
494 stirring and light stimulation induced remarkable shifts in microbial diversity, effective
495 activation on carbon and methane metabolism and the formation of electroactive bio-
496 cluster. During 90-day polit-scale operation, the proposed homogenous-illuminated

system demonstrated the superior $CH_4$ yield and carbon removal under high ammonia stress. From an economic standpoint, the naturally viable solar illumination with optimized intermittent mixing could minimize energy demand and maintenance cost in full-scale application, presenting a sustainable and easy-operated treatment approach for efficient waste-to-energy recovery.

**Acknowledgements**

This research was supported by Scientific Research (B) 22H03778 and Grant-in-Aid for Exploratory Research 21k19628 from Japan Society for the Promotion of Science. The Figure 5c in the paper was drawn using Figdraw platform (www.figdraw.com).

**Appendix A. Supplementary data**

E-supplementary data of this work can be found in online version of the paper.

**Reference**

Babiak, W., Krzemińska, I., 2021. Extracellular polymeric substances (EPS) as microalgal bioproducts: A review of factors affecting EPS synthesis and application in flocculation processes. Energies 14, 4007. https://doi.org/10.3390/en14134007

Bose, R.S., Chowdhury, B., Zakaria, B.S., Kumar Tiwari, M., Ranjan Dhar, B., 2021. Significance of different mixing conditions on performance and microbial communities in anaerobic digester amended with granular and powdered activated carbon. Bioresour. Technol. 341, 125768.

https://doi.org/10.1016/j.biortech.2021.125768

Dang, H., Yu, N., Mou, A., Zhang, L., Guo, B., Liu, Y., 2022. Metagenomic insights into direct interspecies electron transfer and quorum sensing in blackwater anaerobic digestion reactors supplemented with granular activated carbon. Bioresour. Technol. 352, 127113. https://doi.org/10.1016/J.BIORTECH.2022.127113

Dyksma, S., Jansen, L., Gallert, C., 2020. Syntrophic acetate oxidation replaces acetoclastic methanogenesis during thermophilic digestion of biowaste. Microbiome 8(1), 1–14. https://doi.org/10.1186/s40168-020-00862-5

Fischer, M.A., Ulbricht, A., Neulinger, S.C., Refai, S., Waßmann, K., Künzel, S., Schmitz, R.A., 2019. Immediate Effects of Ammonia Shock on Transcription and Composition of a Biogas Reactor Microbiome. Front. Microbiol. 10, 2064. https://doi.org/10.3389/fmicb.2019.02064

Haig, S.J., Quince, C., Davies, R.L., Dorea, C.C., Collinsa, G., 2015. The relationship between microbial community evenness and function in slow sand filters. MBio 6, e00729-15. https://doi.org/10.1128/mBio.00729-15

Hattori, S., 2008. Syntrophic acetate-oxidizing microbes in methanogenic environments. Microbes Environ. https://doi.org/10.1264/jsme2.23.118

He, Z.W., Yang, C.X., Tang, C.C., Liu, W.Z., Zhou, A.J., Ren, Y.X., Wang, A.J., 2021. Response of anaerobic digestion of waste activated sludge to residual ferric ions. Bioresour. Technol. 322, 124536.

https://doi.org/10.1016/J.BIORTECH.2020.124536

Karim, K., Hoffmann, R., Klasson, T., Al-Dahhan, M.H., 2005. Anaerobic digestion of animal waste: Waste strength versus impact of mixing. Bioresour. Technol. 96, 1771–1781. https://doi.org/10.1016/j.biortech.2005.01.020

Kariyama, I.D., Zhai, X., Wu, B., 2018. Influence of mixing on anaerobic digestion efficiency in stirred tank digesters: A review. https://doi.org/10.1016/j.watres.2018.06.065

Kowalczyk, A., Harnisch, E., Schwede, S., Gerber, M., Span, R., 2013. Different mixing modes for biogas plants using energy crops. Appl. Energy 112, 465–472. https://doi.org/10.1016/J.APENERGY.2013.03.065

Lembo, G., Rosa, S., Miritana, V.M., Marone, A., Massini, G., Fenice, M., Signorini, A., 2020. Thermophilic anaerobic digestion of second cheese whey: microbial community response to H2 addition in a partially immobilized anaerobic hybrid reactor. Process. 2021, Vol. 9, Page 43 9, 43. https://doi.org/10.3390/PR9010043

Li, L., Wang, K., Sun, Z., Zhao, Q., Zhou, H., Gao, Q., Jiang, J., Mei, W., 2022. Effect of optimized intermittent mixing during high-solids anaerobic co-digestion of food waste and sewage sludge: Simulation, performance, and mechanisms. Sci. Total Environ. 842, 156882. https://doi.org/10.1016/J.SCITOTENV.2022.156882

Lindmark, J., Eriksson, P., Thorin, E., 2014a. The effects of different mixing intensities during anaerobic digestion of the organic fraction of municipal solid waste. Waste Manag. 34, 1391–1397. https://doi.org/10.1016/J.WASMAN.2014.04.006

Lindmark, J., Thorin, E., Bel Fdhila, R., Dahlquist, E., 2014b. Effects of mixing on the result of anaerobic digestion: Review. Renew. Sustain. Energy Rev. https://doi.org/10.1016/J.RSER.2014.07.182

Liu, Y., Wang, X., Sun, Y., 2024. Optimization and experimental study of variable frequency intermittent stirring strategy for anaerobic digestion based on CFD. Fuel 355, 129371. https://doi.org/10.1016/J.FUEL.2023.129371

Liu, Z., Zhu, Y., Zhao, C., Zhang, C., Ming, J., Sharma, A., Chen, G., Yang, Y., 2022. Light stimulation strategy for promoting bio-hydrogen production: Microbial community, metabolic pathway and long-term application. Bioresour. Technol. 350, 126902. https://doi.org/10.1016/j.biortech.2022.126902

Nielfa, A., Cano, R., Fdz-Polanco, M., 2015. Theoretical methane production generated by the co-digestion of organic fraction municipal solid waste and biological sludge. Biotechnol. Reports 5, 14–21. https://doi.org/10.1016/J.BTRE.2014.10.005

Oliver, T.H., Heard, M.S., Isaac, N.J.B., Roy, D.B., Procter, D., Eigenbrod, F., Freckleton, R., Hector, A., Orme, C.D.L., Petchey, O.L., Proença, V., Raffaelli, D., Suttle, K.B., Mace, G.M., Martín-López, B., Woodcock, B.A., Bullock, J.M., 2015. Biodiversity and Resilience of Ecosystem Functions. Trends Ecol. Evol. 30, 673–684. https://doi.org/10.1016/J.TREE.2015.08.009

Ong, H.K., Greenfield, P.F., Pullammanappallil, P.C., 2002. Effect of mixing on biomethanation of cattle-manure slurry. Environ. Technol. 23, 1081–1090. https://doi.org/10.1080/09593332308618330

581 Qian, J., Zhang, Y., Wang, P., Lu, B., He, Y., Tang, S., Yi, Z., 2022. Light alters
582 microbiota and electron transport: Evidence for enhanced mesophilic digestion of
583 municipal sludge. Water Res. 217, 118447.
584 https://doi.org/10.1016/j.watres.2022.118447
585 Rajagopal, R., Massé, D.I., Singh, G., 2013. A critical review on inhibition of anaerobic
586 digestion process by excess ammonia. Bioresour. Technol. 143, 632–641.
587 https://doi.org/10.1016/J.BIORTECH.2013.06.030
588 Rossi, S., Sforza, E., Pastore, M., Bellucci, M., Casagli, F., Marazzi, F., Ficara, E., 2020.
589 Photo-respirometry to shed light on microalgae-bacteria consortia—a review. Rev.
590 Environ. Sci. Biotechnol. 19, 43–72. https://doi.org/10.1007/s11157-020-09524-2
591 Tada, C., Tsukahara, K., Sawayama, S., 2006. Illumination enhances methane
592 production from thermophilic anaerobic digestion. Appl. Microbiol. Biotechnol. 71,
593 363–368. https://doi.org/10.1007/s00253-005-0146-z
594 Tian, H., Fotidis, I.A., Mancini, E., Treu, L., Mahdy, A., Ballesteros, M., González-
595 Fernández, C., Angelidaki, I., 2018. Acclimation to extremely high ammonia levels
596 in continuous biomethanation process and the associated microbial community
597 dynamics. Bioresour. Technol. 247, 616–623.
598 https://doi.org/10.1016/J.BIORTECH.2017.09.148
599 Wang, Caiqin, Wang, Chen, Liu, J., Xu, Q., Han, Z., Xu, X., Zhu, L., 2020. Tolerance
600 of Aceticlastic Methanogenesis Enhanced by Magnetite under the Condition of
601 Ammonia Stress. ACS Sustain. Chem. Eng. 8, 1417–1426.

https://doi.org/10.1021/acssuschemeng.9b05585

Yan, W., Lu, D., Liu, J., Zhou, Y., 2019. The interactive effects of ammonia and carbon nanotube on anaerobic digestion. Chem. Eng. J. 372, 332–340. https://doi.org/10.1016/J.CEJ.2019.04.163

Yoon, S.H., Ha, S.M., Kwon, S., Lim, J., Kim, Y., Seo, H., Chun, J., 2017. Introducing EzBioCloud: A taxonomically united database of 16S rRNA gene sequences and whole-genome assemblies. Int. J. Syst. Evol. Microbiol. 67, 1613–1617. https://doi.org/10.1099/ijsem.0.001755

Zhang, N., Stanislaus, M.S., Hu, X., Zhao, C., Zhu, Q., Li, D., Yang, Y., 2016. Strategy of mitigating ammonium-rich waste inhibition on anaerobic digestion by using illuminated bio-zeolite fixed-bed process. Bioresour. Technol. 222, 59–65. https://doi.org/10.1016/j.biortech.2016.09.053

Zhao, Z., Wang, J., Li, Y., Zhu, T., Yu, Q., Wang, T., Liang, S., Zhang, Y., 2020. Why do DIETers like drinking: Metagenomic analysis for methane and energy metabolism during anaerobic digestion with ethanol. Water Res. 171, 115425. https://doi.org/10.1016/j.watres.2019.115425

Zheng, H., Sharma, A., Ma, Q., Zhang, C., Hiranuma, T., Chen, Y., Chen, G., Yang, Y., 2020. Development of an oyster shell and lignite modified zeolite (OLMZ) fixed bioreactor coupled with intermittent light stimulation for high efficient ammonium-rich anaerobic digestion process. Chem. Eng. J. 398, 161. https://doi.org/10.1016/j.cej.2020.125637

623 Zheng, Z., Cai, Y., Zhang, Y., Zhao, Y., Gao, Y., Cui, Z., Hu, Y., Wang, X., 2021. The
624 effects of C/N (10–25) on the relationship of substrates, metabolites, and
625 microorganisms in “inhibited steady-state” of anaerobic digestion. Water Res. 188,
626 116466. https://doi.org/10.1016/j.watres.2020.116466
627 Zhu, Y., Liu, Z., Zhang, C., Ming, J., Chen, G., Yang, Y., 2022. Light triggers green
628 recovery: Boosted biomethane production from ammonia-stressed anaerobic
629 digestion through optimized illuminated bioreactor. Chem. Eng. J. 450, 138173.
630 https://doi.org/10.1016/j.cej.2022.138173
631 Zhu, Y., Zhang, N., Liu, Z., Liu, N., Sharma, A., Chen, G., Yang, Y., 2021. Photon
632 number based anaerobic digestion process for efficient bio-methane conversion
633 from ammonium-rich feedstock: Performance evaluation and practical potential.
634 Energy Convers. Manag. 238, 114155.
635 https://doi.org/10.1016/J.ENCONMAN.2021.114155
636

**Table 1** Semi-continuous AD performance during different characteristic stages at pilot scale under ammonia stress

| Parameter \ Stage | Dark | Light | Light-$S_{opt}$ | | |
|---|---|---|---|---|---|
| Period | Day 0-20 | Day 21-50 | Day 51-70 | Day 71-80 | Day 81-90 |
| OLR (g-$DOC_{added}$/(L·d)) | 0.19 | 0.19 | 0.19 | 0.34 | 0.71 |
| C/N | 0.31 | 0.31 | 0.31 | 0.38 | 0.56 |
| HRT (day) | 10 | 10 | 10 | 5 | 5 |
| DOC removal efficiency (%) | 80.6 | 83.1 | 85.3 | 84.3 | 81.6 |
| Average daily $CH_4$ yield (mL/(g-$DOC_{removal}$·d)) | 781 ± 26 | 877 ± 36 | 914 ± 31 | 953 ± 35 | 971 ± 29 |

Figure

Click here to access/download;Figure;Figures1.docx

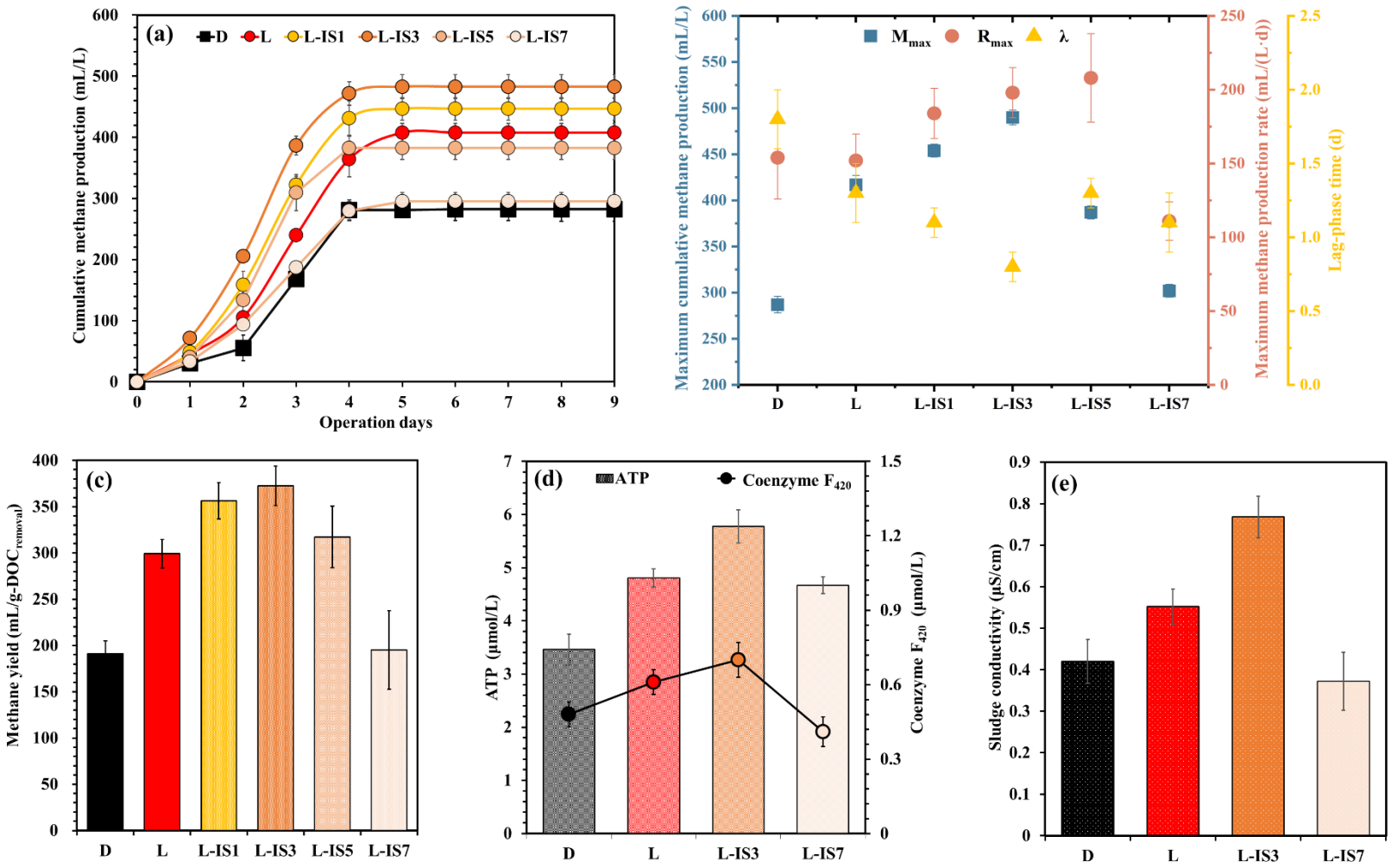


**Fig. 1** Methane performance of **(a)** cumulative methane production, **(b)** maximal cumulative $CH_4$ production, maximal $CH_4$ production rate and lag-phase time fitted with Gompertz model, and **(c)** methane yield, and microbial activity indicators of **(d)** ATP and coenzyme $F_{420}$, and **(e)** sludge conductivity in bioreactors under different stirring conditions during batch experiment. (Error bars designate standard deviations of triplicate experiments)

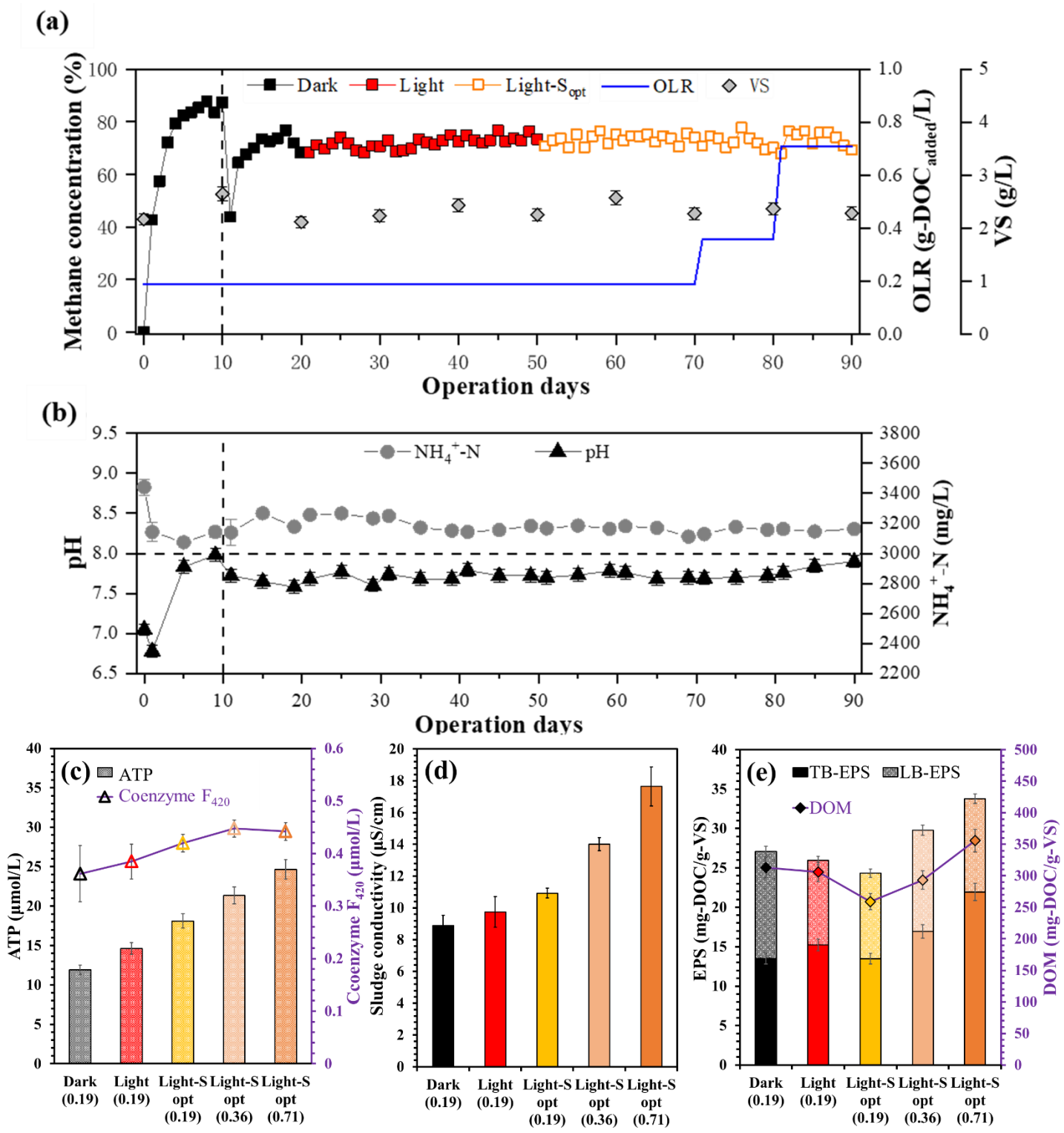


**Fig. 2** Long-term performance of pilot-scale bio-fixed bed digester under dark (Dark), illumination (Light) and homogenous illumination (Light-S $_{opt}$) with different OLR. **(a)** Variations of $CH_4$ concentration and biomass quantity, **(b)** variations of pH and $NH_4^+$-N, **(c)** average levels of ATP, coenzyme $F_{420}$ and **(d)** sludge conductance, and **(e)** EPS components of sludge. (Error bars designate standard deviations of triplicate experiments)

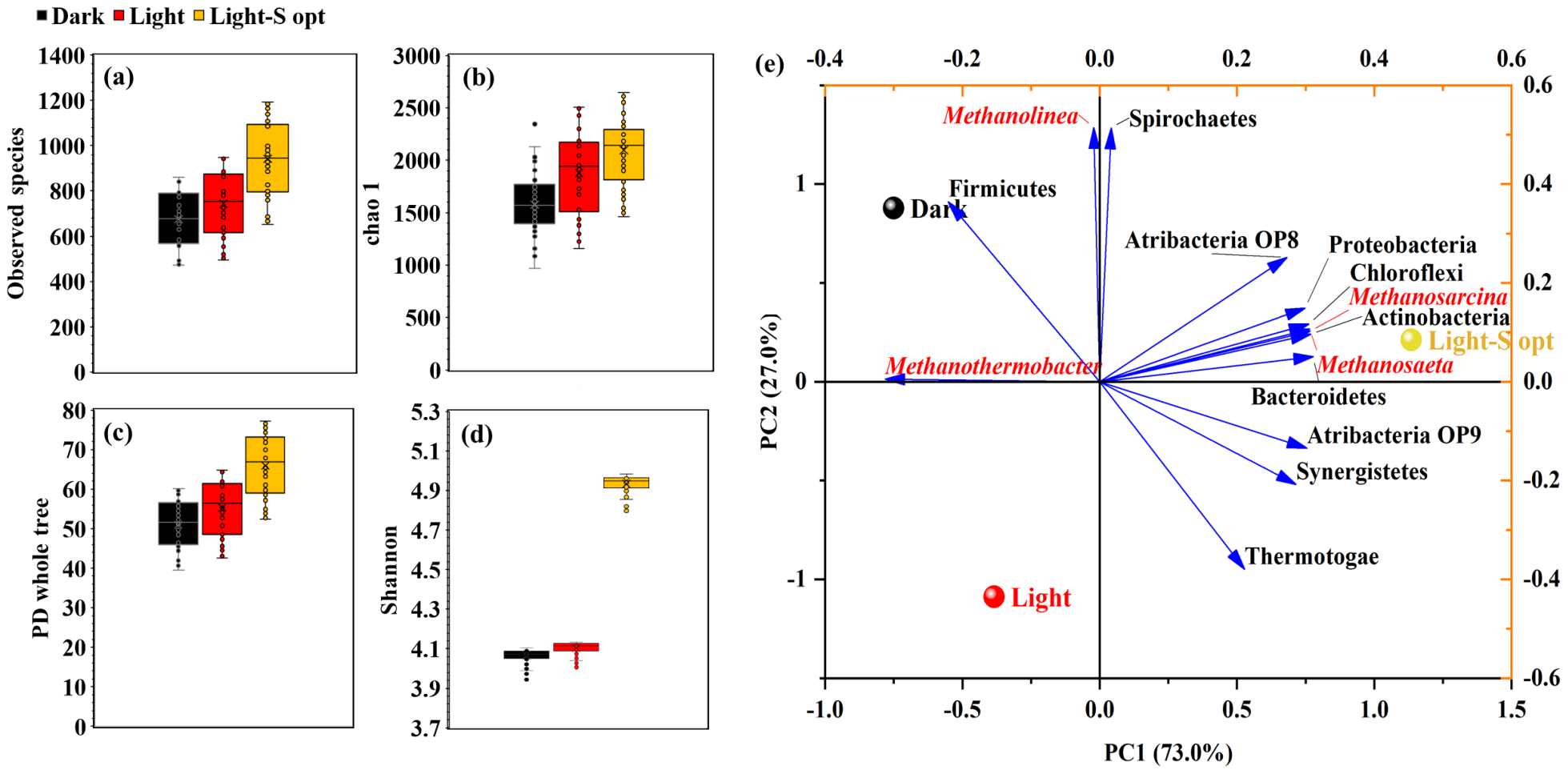


**Fig. 3** Boxplots for microbial richness and diversity with indexes of **(a)** observed species, **(b)** Chao1, **(c)** PD whole tree and **(d)** Shannon; and **(e)** PCA plot depicted dominant microbial populations (bacterial order and archaeal genera) during each stage in long-term operation.

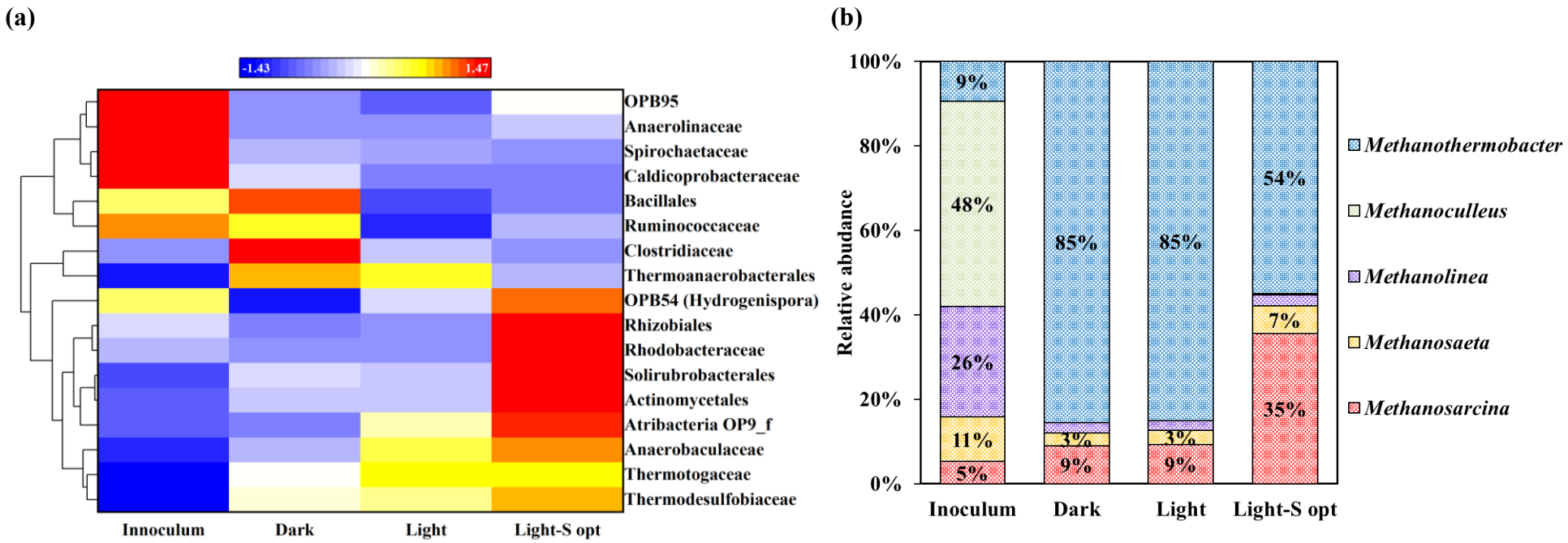


**Fig. 4 (a)** Heat map with cluster analysis of dominant bacterial family, and **(b)** relative abundance of methanogenic genera from original inoculum, Dark stage, Light stage and Light-S $_{opt}$ stages.

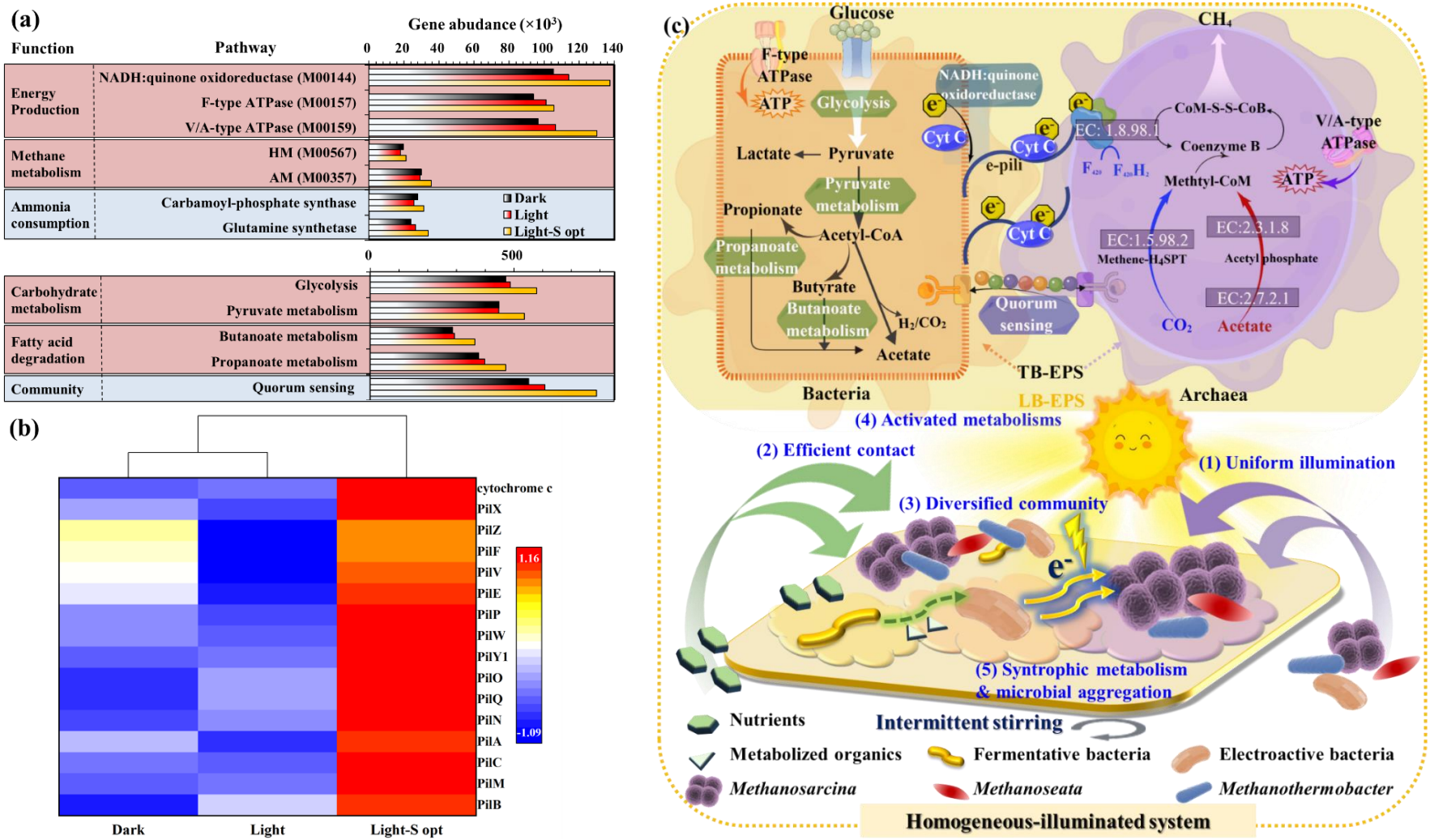


**Fig. 5 (a)** Gene copy numbers of key metabolic pathways from each stage during pilot-scale operation, and **(b)** heat map of genes abundance involved in cytochrome c and e-pili accessory proteins (pilA, pilB, pilC, pilE, pilF, pilM, pilN, pilO, pilP, pilQ, pilV, pilW, pilX pilY1 and pilZ), and **(c)** conceptual graph of mechanisms in homogenous-illuminated biosystem for enhanced ammonia-rich AD performance.